ACS Sustainable Chemistry & Engineering

Research Article

pubs.acs.org/journal/ascecg

# Three-Dimensional Macroporous Graphene Foam Filled with Mesoporous Polyaniline Network for High Areal Capacitance

Jintao Zhang, Jing Wang, Jien Yang, Yilei Wang, and Mary B. Chan-Park*

School of Chemical and Biomedical Engineering, Nanyang Technological University, 62 Nanyang Drive, Singapore 637459

Supporting Information

**ABSTRACT:** Bicontinuous macroporous graphene foam composed of few-layered graphene sheets provides a highly conductive platform on which to deposit mesoporous polyaniline via incorporation of electrodeposition and inkjet techniques. The experimental results exhibit that the coating polyaniline thin layer on the surface of three-dimensional graphene foam via electrodeposition is of importance for changing the hydrophobic surface to a hydrophilic one and for the subsequent filling of the mesoporous polyaniline network into the macroporous graphene foam. The porous polyaniline network with high pseudocapacitance is highly efficient for adjusting the pore structure and capacitive properties of graphene foam. When used as electrode materials for supercapacitors, the resulted graphene foam−polyaniline network with high porosity renders a large areal capacitance of over 1700 mF $cm^{-2}$, which is over two times the enhancement in comparison with the pure graphene foam and polyaniline thin layer coated one. The ultrahigh areal capacitance benefits from the synergistic effect of the good conductive graphene backbone and high pseudocapacitive polyaniline.

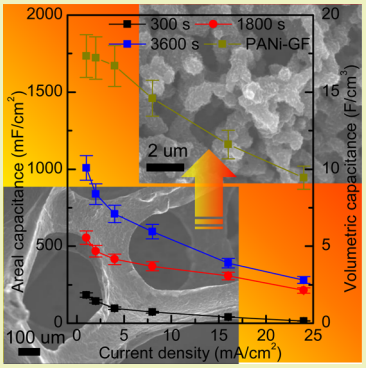


**KEYWORDS:** *Graphene, Polyaniline, Supercapacitor, Porous structure, Areal capacitance*

## INTRODUCTION

The increasing demand for clean energy storage and applications has motivated recent research efforts into the development of supercapacitors with both high energy and power density through exploitation of advanced electrode materials.[1,2] Graphene-based materials are considered to be potential electrode materials for next-generation supercapacitors because of their large specific surface area, good electrical conductivity, and chemical and thermal stability.[3−5] The high mechanical strength and flexibility of this atomically thin two-dimensional carbon material makes graphene particularly attractive to fabricate light and flexible supercapacitors.[6−11] The chemically reduced graphene oxide (RGO) opens new ways to prepare graphene-based electrodes for supercapacitor applications.[12−16] However, RGO sheets prefer to restack together due to strong $\pi-\pi$ interactions, leading to well restacked and conductive graphene films.[17,18] In supercapacitor electrodes, this material leads to inferior capacitance due to the poor penetration of electrolytes into the compact structure of the RGO film. The shortage would be eliminated by fabricating RGO-based materials with high surface area via rationally designed methods,[7,13,19−23] such as template methods.[24]

Alternatively, ultrathin graphene foam consisting of a few layers of graphene can be prepared by chemical vapor deposition templating nickel foam.[22,25] The lack of intrinsic electrochemical activity of graphene materials limits their capacitive performance. The macro-sized pores (around several hundreds of micrometres) are efficient to facilitate electrolyte transfer but do not contribute to the areal capacitance. Nevertheless, graphene foam provides an excellent platform with high electric conductivity and porosity on which to deposit various metal oxides and conducting polymers for various electrochemical applications.[26−28] It is still challenging to prepare graphene-based supercapacitor electrodes with large areal capacitance.[29,30] Anodic electropolymerization of polyaniline (PANi) on macroporous graphene foam gave an enhanced specific capacitance benefiting from the large pseudocapacitive contribution of PANi. The shortcoming is that only a thin layer of metal oxide or conducting polymers has been coated on the surface of graphene foam,[31,32] resulting in small areal capacitance. Thus, it is highly desirable to fill the macro-sized pores with pseudocapacitive material with smaller pores in order to boost its areal capacitance.[33]

Herein, we demonstrate a simple approach to filling macroporous graphene foam with mesoporous PANi via the combination of electrodeposition and subsequent oxidative polymerization of aniline monomers. The approach is robust not only to adjust the pore size of graphene foam but also to introduce pseudocapacitive materials. When used as electrode materials for supercapacitors, the bicontinuous graphene foam is an efficient backbone for facile electron transfer, while the mesoporous PANi can provide large pseudocapacitance. Thus, high areal capacitance has been achieved.

**Received:** April 10, 2014
**Revised:** August 24, 2014
**Published:** August 29, 2014

   dx.doi.org/10.1021/sc500247h | *ACS Sustainable Chem. Eng.* 2014, 2, 2291−2296

## EXPERIMENTAL SECTION

**Preparation of Polyaniline-Filled Graphene Foam.** Three-dimensional (3D) graphene foam was synthesized by a modified chemical vapor deposition (CVD) method with nickel foam as the growth substrate and ethanol as the precursor under atmospheric pressure according to previous reports.[22,25] Typically, the nickel foam placed into a quartz tube was heated to 1000 °C at a 50 °C/min heating rate and maintained for 10 min under atmospheric pressure with a gas flow of $H_2$/Ar ($H_2$/Ar = 25:50 sccm) to clean the surface of the nickel foam. After 20 min of growth, the sample is rapidly cooled to room temperature under $H_2$/Ar flow. Finally, the Ni substrate was removed using 3 M HCl at 50 °C for 2 days, leaving free-standing 3D graphene foam. The obtained graphene foam was cut into the designed size and used as an electrode by connecting to a Cu wire with Ag paste. Polyaniline thin films were electrodeposited on the graphene foam (1 cm × 2 cm, thickness ~1.0 mm) in a three-electrode cell with the as-prepared graphene foam as the working electrode, a Pt plate as the counter electrode, and a Ag/AgCl (sat. KCl) electrode as the reference electrode. The electrolyte contained 50 mL of 0.05 M aniline monomers and 0.1 M phytic acid. The electrochemical deposition was performed at a current density of 2 mA $cm^{-2}$ for 300, 1800, and 3600 s at room temperature, respectively. After the coating of graphene foam with a thin layer of polyaniline via electrodeposition for 300 s, 100 uL of aniline monomer and phytic acid with an oxidizing agent ($(NH_4)_2S_2O_8$) was filled into the pores of the polyaniline-coated graphene foam via an inkjet method, and the polymerization was carried out at 4 °C overnight. Finally, the samples were washed with a large amount of DI water, and the obtained sample is named PANi-filled graphene foam.

**Characterization.** The morphology and microstructure of the samples were investigated by field emission scanning electron microscopy (FESEM, JSM-6700F, JEOL, Japan). Fourier transform infrared spectra (FITR) were recorded on a PerkinElmer spectrum GX FTIR system. The Raman spectra were collected by Raman spectroscopy (Renishaw), using a 514 nm laser. The contact angle is measured with a FTA200 dynamic contact angle analyzer. A CHI 760D electrochemical workstation (CH Instruments) was used to measure the electrochemical properties of the samples at ambient temperature (about 22 ∘C). The electrochemical cell had a three-electrode configuration with a bright Pt plate as the counter electrode and an Ag/AgCl electrode as the reference electrode. The as-prepared samples were used as working electrodes. Two M $H_2SO_4$ aqueous solutions were employed as the electrolyte. Cyclic voltammetry (CV, −0.1 to 0.9 V, 10 mV $s^{-1}$) was carried out on an electrochemical workstation (CHI760D). Galvanostatic charging/discharging tests were performed in the potential range of 0 to 0.8 V at different current densities.

## RESULTS AND DISCUSSION

The preparation procedure is illustrated in Figure 1. Graphene foam is synthesized via chemical vapor deposition according to the previous reports.[22,25] PANi thin film is first coated on graphene foam by a galvanostatic electropolymerization method at a current density of 2 mA/$cm^2$. Then, aniline monomers are inkjet printed into the pores of the PANi-coated graphene foam and subsequently oxidative polymerized to porous PANi hydrogel with the help of phytic acid. Phytic acid characterized by a high density of phosphate groups are able to interact with PANi chains, guiding the formation of porous PANi hydrogel.[34] The inkjet method is effective to fill the aniline monomer with a defined volume into the pores of graphene foam in order to regulate the loading of porous PANi. Figure 2a shows the morphology of 3D graphene foam, exhibiting a well-defined macroporous structure with a pore diameter of ~100−400 $\mu$m, and the pore−ligament structure is similar to that of the Ni foam due to the conformal chemical vapor deposition growth. The enlarged SEM image reveals that the graphene scaffold has a smooth surface (Figure 2b). After electrochemical deposition of PANi for 300 and 1800 s (Figure 2c−f), the open pore structure is preserved, but the graphene surface is covered with an increasingly dense PANi layer with few nanorods (Figure 2f), indicating the increased loading of PANi. When the deposition time is increased to 3600 s (Figure 2g,h), the graphene scaffold is covered with dendritic PANi microstructures. When the phytic acid in the electrolyte is replaced with sulfinic acid, PANi nanofibers with a diameter of about 80 nm are deposited on the surface of the graphene foam (Figure S1, Supporting Information), suggesting that acid plays an important role in the growth of the PANi nanostructure.

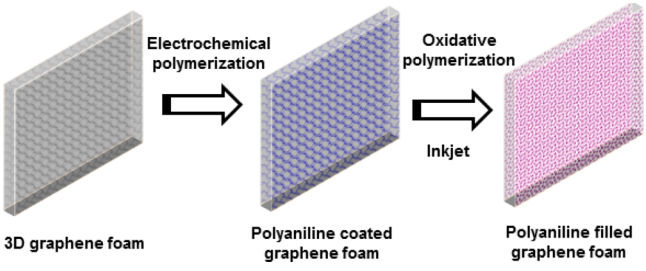


**Figure 1.** Illustration for the preparation procedure of polyaniline-filled graphene foam via a two-step method.

Figure 3a shows the typical Raman spectra of graphene foam and PANi-coated graphene foam. The graphene foam exhibits G and 2D peaks at ~1580 and ~2712 $cm^{-1}$, which is consistent with the literature.[22,25,35] The absence of the D band suggests the formation of high quality and uniform graphene sheets almost without the disordered structural defects. The area ratio of the 2D and G bands suggests that the as-prepared graphene foams are mainly composed of few-layered graphene.[22,25] For the PANi-coated graphene foam sample, in addition to the 2D and G bands, other bands at about 1160 and 1335 $cm^{-1}$ ascribed to the C−H vibrations in quinoid/phenyl groups and the semiquinone radical cation structure in PANi suggests the formation of PANi coating.[36] Figure 3b shows FTIR spectra of graphene foam and PANi-coated graphene foam. The nearly featureless FTIR spectrum of graphene foam, with only a band at about 1630 $cm^{-1}$ corresponding to the skeletal vibration of graphene sheet, suggests that the surfaces of the graphene sheets have few functional groups. In contrast, many sharp peaks are observed for the sample of PANi-coated graphene foam. Specifically, the typical bands at 1565 and 1475 $cm^{-1}$ are assigned to C═C stretching vibration modes in quinoid and benzene rings, respectively, whereas the bands at 1299 and 1240 $cm^{-1}$ are related to the C−N and C═N stretching modes, respectively.[37] The presence of these bands suggests the successful deposition of PANi on the graphene foam. Additionally, the bands at around 1100 and 800 $cm^{-1}$ are attributed to the C−H in-plane bending and the C−H out-of-plane bending modes, respectively. As shown in Figure S2a of the Supporting Information, the large contact angle of 139° clearly indicates the hydrophobicity of graphene foam. In contrast, the continuous optical images exhibit that the water droplet is soaked immediately into the PANi-coated graphene foam, suggesting a superhydrophilic nature. The results exhibit that the coating of PANi on the graphene foam is crucial to imparting a hydrophilic character, which will not only facilitate further deposition of PANi into the pores of the graphene foam but also will allow the electrolyte to be accessed easily.

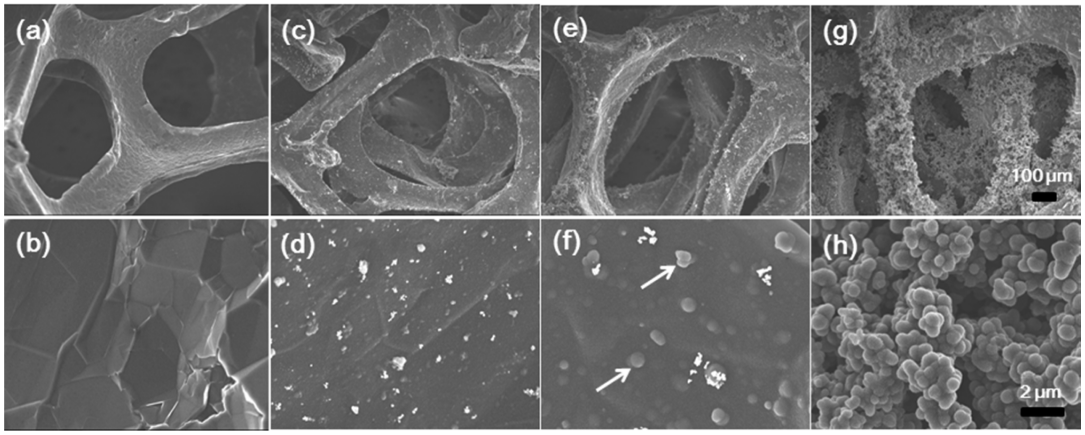


**Figure 2.** SEM images of graphene foam (a) and (b), polyaniline-coated graphene foam via electrochemical polymerization for deposition times of 300 s (c) and (d), 1800 s (e) and (f), and 3600 s (g) and (h).

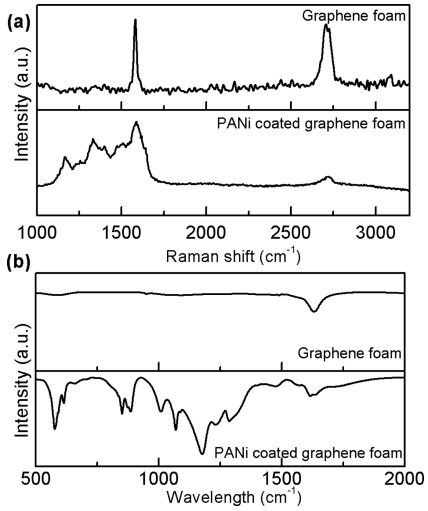


**Figure 3.** Raman spectra (a) and FTIR spectra (b) of graphene foam and PANi-coated graphene foam.

As shown in Figure 4a, the pores of graphene foam with a PANi thin layer can be further filled with porous PANi via oxidative polymerization of an aniline monomer among the macro-sized pores. In the presence of phytic acid, aniline monomers are polymerized to form a porous PANi hydrogel.[34]

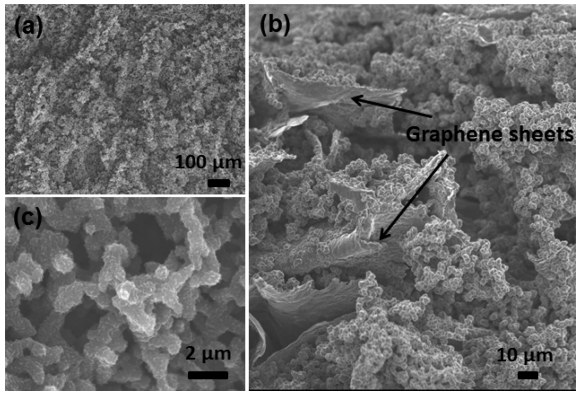


**Figure 4.** SEM image (a), cross-section SEM image (b), and enlarged SEM image (c) of graphene foam filled with polyaniline via oxidative polymerization.

In the enlarged SEM image (Figure 4b), the PANi aerogel exhibits the interconnected network-like scaffold with a bicontinuous porous structure. The cross-section SEM image reveals that the porous structure of PANi is cross-linked among the pores of graphene foam, which will facilitate electrolyte penetration into the interior for high capacitance. Figure S3 of the Supporting Information reveals the flexible nature of PANi-filled graphene foam, suggesting its potential application in flexible supercapacitors. As a control experiment, the deposition of PANi into the pure graphene foam without PANi coating via electrochemical deposition was also performed. Due to the hydrophobic nature, the pure graphene foam cannot be filled very well (Figure S4, Supporting Information).

The capacitive performance of the samples was characterized using cycle voltammetry (CV) and charge−discharge techniques. The CV curves (Figure 5a) exhibit broad redox peaks, resulting from the pseudocapacitive behavior of PANi, and the current density increases gradually with increasing deposition time. The large area under the CV curve indicates high capacitance because the current is proportional to the capacitance. The electrode exhibits the largest capacitance after filling the graphene foam with the porous PANi network. The charge−discharge curves of the corresponding samples are shown in Figure 5b. All curves exhibit a nearly equilateral triangle shape, suggesting a good reversibility during the charge−discharge processes. The slight voltage plateau is ascribed to the redox behavior of PANi. The good capacitive behaviors of electrode materials can be attributed to the following features: (1) The good hydrophilicity of the samples facilitates the penetration of electrolytes into the inner surface. (2) The good electrical conductivity of the graphene foam facilitates the electron transfer among the electrode material, leading to low internal resistance. (3) The porous PANi filling into the pores of the graphene foam provides large pseudocapacitance on the basis of the redox reactions.

On the basis of the charge−discharge curves at different current densities, the corresponding areal capacitance ($F_s$ in mF cm$^2$ in Figure 5c) is calculated according to the following equation: $F_s=F_g/S$, where $F_g$ (in F g$^{-1}$) is the gravimetric capacitance obtained from the charge−discharge curves and $S$ (in cm$^2$ g$^{-1}$) is the surface area of electrode materials. As shown, the areal capacitance increases with increasing deposition time because more PANi was deposited onto the surface of the graphene foam. The largest areal capacitance for

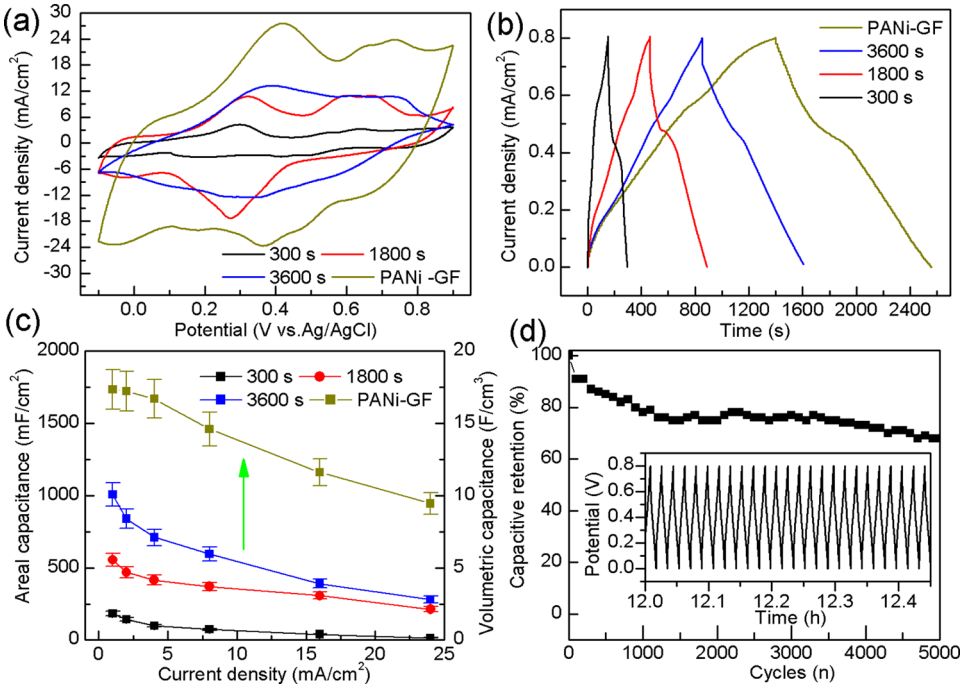


**Figure 5.** Cycle voltammetry curves (a), charge–discharge curves (b), and areal capacitances (c) of PANi-coated graphene foam with different deposition times and PANi-filled graphene foam (PANi-GF). Cycling stability of PANi-GF (d). Inset shows the continuous charge–discharge curves.

PANi-coated graphene foam is over 900 mF $cm^{-2}$. As shown in Figure 2f, there is much space that can be used for PANi deposition after 3600 s of electrodeposition. It can be expected that the areal capacitance would be further increased by filling the pores with porous PANi. Indeed, the areal capacitance of PANi-filled graphene foam is as high as 1700 mF $cm^{-2}$, nearly two times the enhancement in comparison with the PANi-coated graphene foam, and the sample exhibits a good rate performance of ~55% capacitive retention when the current density is increased by 24-fold. The obtained areal capacitance is much higher than those of recently reported graphene-based electrodes, including a PPy-coated RGO electrode (151 mF $cm^{-2}$)[38] and a flexible RGO film-based supercapacitor (4.04 mF $cm^{-2}$).[23] It also outperforms other recently reported supercapacitors based on various pseudocapacitive nanomaterials, such as oriented NiO–$TiO_2$ nanotube arrays (~2.7 mF $cm^{-2}$),[39] highly ordered titania nanotube arrays (~0.9 mF $cm^{-2}$),[40] and $NiCo_2O_4$ nanowire arrays supported on Ni foam (~161 mF $cm^{-2}$).[41] The large areal capacitance of the composite material would contribute to the synergistic effect of the good conductive graphene backbone for rapid electron transfer and the high pseudocapacitive polyaniline with high porosity for easy electrolyte transfer. Cycling stability is tested by repetitive charge–discharge cycles (Figure 5d). The capacitive retention of PANi-filled graphene foam is ~73% after 1500 cycles. However, only a slight decrease is observed during the subsequent cycling test. The capacitive retention is around 69% after 5000 cycles. The capacitive retention is comparable and even higher than those of recently reported results, such as GO/PANi nanocomposite film (53% after 1000 cycles),[42] chemically grafted graphene–PANi composite (68.7% after 1000 cycles),[43] and PANi nanosheets arrayed on GO sheets (62% after 1000 cycles).[44] The porous structure of the PANi-filled graphene foam may be more tolerant to structural changes (e.g., volume expansion) during the charge–discharge process, thus leading to good cycling stability.

## CONCLUSION

In summary, three-dimensional graphene foam composed of ultrathin graphene sheets is used as a highly conductive and porous platform for the deposition of porous polyaniline via electrochemical deposition and oxidative polymerization. The electrodeposition is efficient to coat a thin layer of polyaniline on the surface of the graphene foam and impart a hydrophilic nature, but is not able to fill the large submillimeter-scale pores. The macroporous graphene foam can be totally filled with porous polyaniline via oxidative polymerization in the presence of phytic acid. The porous polyaniline-filled graphene foam exhibits a large areal capacitance of over 1700 mF $cm^{-2}$; over two-fold enhancement of the areal capacitance is achieved in comparison to the graphene foam coated with electrodeposited polyaniline. The good capacitive performance is contributed to the synergic integration between graphene foam and polyaniline. Specifically, the porous graphene foam with good electronic conductivity facilitates the electron transfer among the electrode with low resistance, while the porous polyaniline filled into the graphene foam provides large pseudocapacitance via redox reactions. These unique features endow their promising applications in high-performance supercapacitors.

## ASSOCIATED CONTENT

### Supporting Information

Representative SEM images and optical images. This material is available free of charge via the Internet at http://pubs.acs.org.

## AUTHOR INFORMATION

### Corresponding Author

*E-mail: MBEChan@ntu.edu.sg. Fax: 65 6794 7553. Tel: 65 6790 6064.

### Notes

The authors declare no competing financial interest.

## ■ ACKNOWLEDGMENTS

This work was supported by a Competitive Research Program grant from the Singapore National Research Foundation (NRF-CRP2-2007-02).

## ■ REFERENCES

(1) Simon, P.; Gogotsi, Y. Materials for electrochemical capacitors. *Nat. Mater.* **2008**, *7*, 845−854.
(2) Chu, S.; Majumdar, A. Opportunities and challenges for a sustainable energy future. *Nature* **2012**, *488*, 294−303.
(3) Zhang, J.; Zhao, X. On the configuration of supercapacitors for maximizing electrochemical performance. *ChemSusChem* **2012**, *5*, 818−841.
(4) Dai, L. Functionalization of graphene for efficient energy conversion and storage. *Acc. Chem. Res.* **2013**, *46*, 31−42.
(5) Luo, J.; Kim, J.; Huang, J. Material processing of chemically modified graphene: Some challenges and solutions. *Acc. Chem. Res.* **2013**, *46*, 2225−2234.
(6) Gwon, H.; Kim, H. S.; Lee, K. U.; Seo, D. H.; Park, Y. C.; Lee, Y. S.; Ahn, B. T.; Kang, K. Flexible energy storage devices based on graphene paper. *Energy Environ. Sci.* **2011**, *4*, 1277−1283.
(7) Li, C.; Shi, G. Three-dimensional graphene architectures. *Nanoscale* **2012**, *4*, 5549−5563.
(8) Gao, H.; Xiao, F.; Ching, C. B.; Duan, H. Flexible all-solid-state asymmetric supercapacitors based on free-standing carbon nanotube/graphene and $Mn_3O_4$ nanoparticle/graphene paper electrodes. *ACS Appl. Mater. Interfaces* **2012**, *4*, 7020−7026.
(9) Choi, B. G.; Hong, J.; Hong, W. H.; Hammond, P. T.; Park, H. Facilitated ion transport in all-solid-state flexible supercapacitors. *ACS Nano* **2011**, *5*, 7205−7213.
(10) Weng, Z.; Su, Y.; Wang, D.-W.; Li, F.; Du, J.; Cheng, H.-M. Graphene−cellulose paper flexible supercapacitors. *Adv. Energy Mater.* **2011**, *1*, 917−922.
(11) Wu, C.; Huang, X.; Wang, G.; Lv, L.; Chen, G.; Li, G.; Jiang, P. Highly conductive nanocomposites with three-dimensional, compactly interconnected graphene networks via a self-assembly process. *Adv. Funct. Mater.* **2013**, *23*, 506−513.
(12) Li, D.; Muller, M. B.; Gilje, S.; Kaner, R. B.; Wallace, G. G. Processable aqueous dispersions of graphene nanosheets. *Nat. Nano* **2008**, *3*, 101−105.
(13) Liu, F.; Song, S.; Xue, D.; Zhang, H. Folded structured graphene paper for high performance electrode materials. *Adv. Mater.* **2012**, *24*, 1089−1094.
(14) Pei, S.; Zhao, J.; Du, J.; Ren, W.; Cheng, H.-M. Direct reduction of graphene oxide films into highly conductive and flexible graphene films by hydrohalic acids. *Carbon* **2010**, *48*, 4466−4474.
(15) Chen, D.; Tang, L.; Li, J. Graphene-based materials in electrochemistry. *Chem. Soc. Rev.* **2010**, *39*, 3157−3180.
(16) Zhang, L. L.; Zhou, R.; Zhao, X. S. Graphene-based materials as supercapacitor electrodes. *J. Mater. Chem.* **2010**, *20*, 5983−5992.
(17) Stoller, M. D.; Park, S.; Zhu, Y.; An, J.; Ruoff, R. S. Graphene-based ultracapacitors. *Nano Lett.* **2008**, *8*, 3498−3502.
(18) Moon, I. K.; Lee, J.; Ruoff, R. S.; Lee, H. Reduced graphene oxide by chemical graphitization. *Nat. Commun.* **2010**, *1*, 73.
(19) Yu, A.; Roes, I.; Davies, A.; Chen, Z. Ultrathin, transparent, and flexible graphene films for supercapacitor application. *Appl. Phys. Lett.* **2010**, *96*, 253105.
(20) Zhu, Y.; Murali, S.; Stoller, M. D.; Velamakanni, A.; Piner, R. D.; Ruoff, R. S. Microwave assisted exfoliation and reduction of graphite oxide for ultracapacitors. *Carbon* **2010**, *48*, 2118−2122.
(21) Lei, Z.; Liu, Z.; Wang, H.; Sun, X.; Lu, L.; Zhao, X. S. A high-energy-density supercapacitor with graphene-CMK-5 as the electrode and ionic liquid as the electrolyte. *J. Mater. Chem. A* **2013**, *1*, 2313−2321.
(22) Chen, Z.; Ren, W.; Gao, L.; Liu, B.; Pei, S.; Cheng, H.-M. Three-dimensional flexible and conductive interconnected graphene networks grown by chemical vapour deposition. *Nat. Mater.* **2011**, *10*, 424−428.
(23) El-Kady, M. F.; Strong, V.; Dubin, S.; Kaner, R. B. Laser scribing of high-performance and flexible graphene-based electrochemical capacitors. *Science* **2012**, *335*, 1326−1330.
(24) Cao, X.; Yin, Z.; Zhang, H. Three-dimensional graphene materials: Preparation, structures and application in supercapacitors. *Energy Environ. Sci.* **2014**, *7*, 1850.
(25) Dong, X.-C.; Xu, H.; Wang, X.-W.; Huang, Y.-X.; Chan-Park, M. B.; Zhang, H.; Wang, L.-H.; Huang, W.; Chen, P. 3D Graphene−cobalt oxide electrode for high-performance supercapacitor and enzymeless glucose detection. *ACS Nano* **2012**, *6*, 3206−3213.
(26) Liu, J.; Lv, W.; Wei, W.; Zhang, C.; Li, Z.; Li, B.; Kang, F.; Yang, Q.-H. A three-dimensional graphene skeleton as a fast electron and ion transport network for electrochemical applications. *J. Mater. Chem. A* **2014**, *2*, 3031−3037.
(27) Wang, H.; Yi, H.; Chen, X.; Wang, X. Asymmetric supercapacitors based on nano-architectured nickel oxide/graphene foam and hierarchical porous nitrogen-doped carbon nanotubes with ultrahigh-rate performance. *J. Mater. Chem. A* **2014**, *2*, 3223−3230.
(28) Luo, J.; Liu, J.; Zeng, Z.; Ng, C. F.; Ma, L.; Zhang, H.; Lin, J.; Shen, Z.; Fan, H. J. Three-dimensional graphene foam supported $Fe_3O_4$ lithium battery anodes with long cycle life and high rate capability. *Nano Lett.* **2013**, *13*, 6136−6143.
(29) Zhang, G.; Lou, X. W. General solution growth of mesoporous $NiCo_2O_4$ nanosheets on various conductive substrates as high-performance electrodes for supercapacitors. *Adv. Mater.* **2013**, *25*, 976−979.
(30) Zhang, G. Q.; Wu, H. B.; Hoster, H. E.; Chan-Park, M. B.; Lou, X. W. Single-crystalline $NiCo_2O_4$ nanoneedle arrays grown on conductive substrates as binder-free electrodes for high-performance supercapacitors. *Energy Environ. Sci.* **2012**, *5*, 9453−9456.
(31) Wang, D.-W.; Li, F.; Zhao, J.; Ren, W.; Chen, Z.-G.; Tan, J.; Wu, Z.-S.; Gentle, I.; Lu, G. Q.; Cheng, H.-M. Fabrication of graphene/polyaniline composite paper via in situ anodic electropolymerization for high-performance flexible electrode. *ACS Nano* **2009**, *3*, 1745−1752.
(32) Wang, H.; Casalongue, H. S.; Liang, Y.; Dai, H. $Ni(OH)_2$ nanoplates grown on graphene as advanced electrochemical pseudocapacitor materials. *J. Am. Chem. Soc.* **2010**, *132*, 7472−7477.
(33) Sassin, M. B.; Chervin, C. N.; Rolison, D. R.; Long, J. W. Redox deposition of nanoscale metal oxides on carbon for next-generation electrochemical capacitors. *Acc. Chem. Res.* **2012**, *46*, 1062−1074.
(34) Pan, L.; Yu, G.; Zhai, D.; Lee, H. R.; Zhao, W.; Liu, N.; Wang, H.; Tee, B. C.-K.; Shi, Y.; Cui, Y.; Bao, Z. Hierarchical nanostructured conducting polymer hydrogel with high electrochemical activity. *Proc. Natl. Acad. Sci. U.S.A.* **2012**, *109*, 9287−9292.
(35) Dong, X.; Wang, P.; Fang, W.; Su, C.-Y.; Chen, Y.-H.; Li, L.-J.; Huang, W.; Chen, P. Growth of large-sized graphene thin-films by liquid precursor-based chemical vapor deposition under atmospheric pressure. *Carbon* **2011**, *49*, 3672−3678.
(36) Zhang, J.; Zhao, X. S. Conducting polymers directly coated on reduced graphene oxide sheets as high-performance supercapacitor electrodes. *J. Phys. Chem. C* **2012**, *116*, 5420−5426.
(37) Zhang, J.; Jiang, J.; Li, H.; Zhao, X. S. A high-performance asymmetric supercapacitor fabricated with graphene-based electrodes. *Energy Environ. Sci.* **2011**, *4*, 4009−4015.
(38) Mini, P. A.; Balakrishnan, A.; Nair, S. V.; Subramanian, K. R. V. Highly super capacitive electrodes made of graphene/poly(pyrrole). *Chem. Commun.* **2011**, *47*, 5753−5755.
(39) Kim, J.-H.; Zhu, K.; Yan, Y.; Perkins, C. L.; Frank, A. J. Microstructure and pseudocapacitive properties of electrodes constructed of oriented $NiO-TiO_2$ nanotube arrays. *Nano Lett.* **2010**, *10*, 4099−4104.
(40) Salari, M.; Aboutalebi, S. H.; Konstantinov, K.; Liu, H. K. A highly ordered titania nanotube array as a supercapacitor electrode. *Phys. Chem. Chem. Phys.* **2011**, *13*, 5038−5041.
(41) Wang, Q. F.; Wang, X. F.; Liu, B.; Yu, G.; Hou, X. J.; Chen, D.; Shen, G. Z. $NiCo_2O_4$ nanowire arrays supported on Ni foam for high-performance flexible all-solid-state supercapacitors. *J. Mater. Chem. A* **2013**, *1*, 2468−2473.

(42) Wei, H.; Zhu, J.; Wu, S.; Wei, S.; Guo, Z. Electrochromic polyaniline/graphite oxide nanocomposites with endured electrochemical energy storage. *Polymer* **2013**, *54*, 1820−1831.
(43) Gao, Z.; Wang, F.; Chang, J.; Wu, D.; Wang, X.; Wang, X.; Xu, F.; Gao, S.; Jiang, K. Chemically grafted graphene-polyaniline composite for application in supercapacitor. *Electrochim. Acta* **2014**, *133*, 325−334.
(44) Ning, G.; Li, T.; Yan, J.; Xu, C.; Wei, T.; Fan, Z. Three-dimensional hybrid materials of fish scale-like polyaniline nanosheet arrays on graphene oxide and carbon nanotube for high-performance ultracapacitors. *Carbon* **2013**, *54*, 241−248.